

# Perovskite-type lanthanum chromium-based oxide films prepared by ultrasonic spray pyrolysis

A. FURUSAKI, H. KONNO, R. FURUICHI

*Analytical Laboratory, Faculty of Engineering, Hokkaido University, Kita-Ku, Sapporo-Shi, 060 Japan*

Ultrasonic spray pyrolysis was used to form 2–8  $\mu\text{m}$  thick  $\text{LaCrO}_3$  films on different substrates from  $\text{La}(\text{CrO}_4)(\text{NO}_3) \cdot n\text{H}_2\text{O}$  precursor films. There was an optimum substrate temperature for the formation of uniform precursor films by the spray pyrolysis. When the substrate temperature was lower than 250  $^\circ\text{C}$ , dry precursor films were not formed, while above 250  $^\circ\text{C}$  the deposition rate decreased with substrate temperature. The precursor films were converted to perovskite-type oxide films by heat treatment at 800  $^\circ\text{C}$  in a nitrogen atmosphere. Both A-site substituted ( $\text{La}_{0.8}\text{Ca}_{0.2}$ )  $\text{CrO}_3$  and B-site substituted  $\text{La}(\text{Cr}_{0.5}\text{Mn}_{0.5})\text{O}_3$  oxide films were formed in a similar manner. Electronic conductivity of the oxide films was improved by repetitions of the spray pyrolysis and heat treatment in nitrogen.

## 1. Introduction

Ultrasonic spray pyrolysis is a simple method to prepare submicrometre particles of metals and oxides [1, 2], as well as homogeneous thin films of many oxides and sulphides [3]. The advantages of the method are that the apparatus is uncomplicated and inexpensive (no vacuum system is necessary), and deposition conditions and film composition are easily controlled. Formerly, products made with this method were mostly simple compounds, but recently more complex compounds such as Y–Ba–Cu–O superconducting thin films [4–7], yttrium iron garnet (YIG) thin films [8], calcia-stabilized zirconia (CSZ) thin films [9], and  $\text{La}_{1-x}\text{Sr}_x\text{MnO}_3$  films [10] have been formed.

Perovskite-type  $\text{LaCrO}_3$  has electronic conductivity and is chemically stable at elevated temperatures in oxidizing atmospheres. It is a candidate for separators in solid-oxide fuel cells and also a promising material for high-temperature electrodes. Many methods have been reported to synthesize this compound. In most cases La(III) and Cr(III) compounds were used as starting materials, but Staut and Morgan [11] reported that active precursor powders, which resulted in enhancing the sinterability of  $(\text{La}_{1-x}\text{Sr}_x)\text{CrO}_3$ , were formed by thermal decomposition of complex lanthanum and strontium chromate hydrate intermediates. We reported a method to form  $\text{LaCrO}_3$  [12] and A-site substituted  $(\text{La}_{1-x}\text{M}_x)\text{CrO}_3$  [13, 14] films by electro-deposition from Cr(VI)-based solutions, and also proposed a detailed formation mechanism of  $\text{LaCrO}_3$  from the precursors formed with La(III) and Cr(VI) compounds [15].

In the present work, ultrasonic spray pyrolysis of Cr(VI)-based solutions was applied to the formation of perovskite-type lanthanum chromium-based oxide films.

## 2. Experimental procedure

### 2.1. Formation of precursor films

Quartz glass, alumina, yttria-stabilized zirconia (YSZ), or silicon nitride plates ( $10 \times 20 \times 1$  or  $25 \times 25 \times 1$   $\text{mm}^3$ ) were used as substrates after degreasing in toluene and acetone. The substrate was set on a stainless steel plate (60 mm diameter  $\times$  2 mm) and heated at 200–700  $^\circ\text{C}$ . Stoichiometric solutions of 0.025–0.25  $\text{mol dm}^{-3}$  were prepared by dissolving appropriate amounts of lanthanum nitrate, calcium nitrate, manganese (II) nitrate, and chromium trioxide in distilled water. The solutions were nebulized at about 100  $\text{cm}^3 \text{h}^{-1}$  with an ultrasonic atomizer which was operated at 1.7 MHz. The average diameter of the generated microscopic droplets was calculated to be about 20  $\mu\text{m}$ . The mist was transported by air to the heated substrate for 30–120 min to form precursor films.

The structure and morphology of the precursor films were examined by X-ray diffraction (XRD) with  $\text{CuK}_\alpha$  radiation and a scanning electron microscope (SEM). The precursor films were dissolved in a dilute nitric acid solution and the amounts of metal ions were analysed by inductively coupled plasma atomic emission spectrometry (ICP–AES). Powder scraped from the substrate was examined by thermogravimetry (TG; at 10  $\text{K min}^{-1}$  in a nitrogen flow of 30  $\text{cm}^3 \text{min}^{-1}$ ), differential thermal analysis (DTA), infrared spectroscopy (IR; by the KBr method), and elemental analysis.

### 2.2. Heat treatment of the precursor films and characterization of oxide films

Perovskite-type oxide films were formed by heat treatment of the precursor films at 800  $^\circ\text{C}$  for 30 min (non-substituted and B-site manganese-substituted types) and at 1000  $^\circ\text{C}$  for 30 min (A-site calcium-substituted

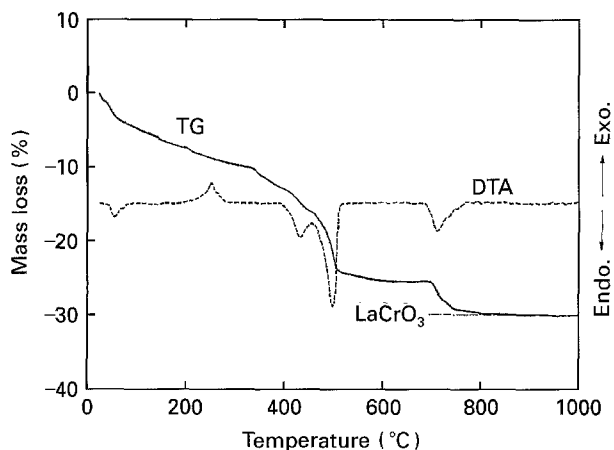


Figure 1 The TG-DTA curves of the La(III)-Cr(VI) precursor film deposited at 400 °C for 60 min on quartz glass.

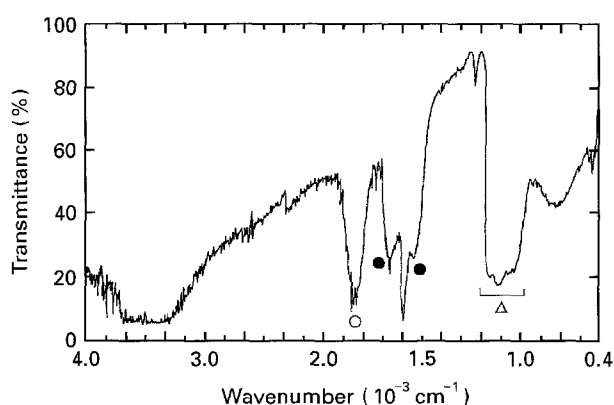


Figure 2 Infrared spectrum of the La(III)-Cr(VI) precursor film deposited at 400 °C for 60 min on quartz glass. (○) Water of crystallization, (●) nitrate ions, (Δ) chromate ions.

type) in a nitrogen atmosphere. In addition to the one-cycle formation by spray pyrolysis and heat treatment, three-cycle formation was also carried out to examine how repeated formation affects the electronic conductivity of the films. The structure and morphology of the oxide films were examined by XRD and SEM, and the thickness was estimated by SEM on film cross-sections. Conductivity was measured in air at different temperatures by the d.c. four-probe method, using platinum paste as current and voltage terminals. Constant voltage ( $E = 40 \text{ V}$ ) was used in the low-conductivity region and constant current ( $I = 1 \mu\text{A} - 50 \text{ mA}$ ) in the high-conductivity region.

### 3. Results and discussion

#### 3.1. Formation of precursor films

There was a limiting substrate temperature for the deposition of dry precursor films, between 250 and 350 °C depending on the precursor species. The atomic ratios of La(:Ca):Cr(:Mn) in the precursor films agreed well with those in the starting solutions, and they were independent of the formation conditions such as substrate temperature, spraying time, and solution concentration. This suggests that the film composition is easily controlled in this method.

Fig. 1 shows TG-DTA curves of the La(III)-Cr(VI) precursor powder obtained by scraping the film from a quartz plate. The precursor has a formula weight of  $340 \pm 5$ , and is considered to be  $\text{La}(\text{CrO}_4)(\text{NO}_3) \cdot n\text{H}_2\text{O}$  ( $n \approx 1.5$ ) from the results of IR measurements and the elemental analysis described below. A plateau at about 600 °C on the TG curve corresponds to the formation of  $\text{LaCrO}_4$  as an intermediate [15, 16]. The DTA curve shows four major endothermic peaks at 55, 434, 500 and 710 °C, and one exothermic peak at 250 °C. The first endothermic peak at 55 °C is due to dehydration, the second and the third correspond to decomposition of nitrate ions, and the fourth arises from deoxidizing and phase transition from  $\text{LaCrO}_4$  to  $\text{LaCrO}_3$ . It was not possible to assign an explanation for the exothermic peak at 250 °C. As shown in Fig. 2, the IR spectrum of the same sample indicates the presence of water of crystallization ( $1660 \text{ cm}^{-1}$ ), nitrate ions ( $1490$  and  $1370 \text{ cm}^{-1}$ ) and chromate ions ( $780 - 980 \text{ cm}^{-1}$ ). The nitrogen content of this precursor was 3.06% and almost consistent with the above composition.

The amount of metal ions in the precursor films increased proportionally with spraying time and solution concentration, and decreased with substrate temperature. With prolonged spraying time, over 120 min, the surface became powder-like. The effects of substrate temperatures and spraying time on the structure of precursor films formed on quartz glass are shown in Fig. 3a and b. Below 300 °C the precursor films are amorphous, and above 400 °C they are crystallized. The patterns indicate a slight expansion of the crystal lattice above 550 °C and the perovskite oxide phase ( $2\theta = 32.6^\circ$ ) is also formed. The diffraction peaks in Fig. 3a were not observed in the case of powder precursors, and the peak intensities decreased drastically with YSZ and alumina substrates. These peaks could not be assigned to known compounds, but it is considered that the observed structures are characteristic of thin films and that the patterns are influenced by substrate species. The intensity of diffraction peaks decreases with spraying time (Fig. 3b) showing that the precursor films do not grow epitaxially.

#### 3.2. Heat treatment of perovskite-type oxide films

The precursor films formed on quartz glass were heated under the conditions described in Section 2.2 and the XRD patterns of the formed oxide films are shown in Fig. 4. With all samples, only the diffraction peaks for the perovskite-type oxides are observed, and the patterns were similar to those of powder diffraction [17]. As shown in Table I, differences in lattice constants between film and powder [18, 19] are not significant, and there are few effects of substitutions on the lattice sizes.

Surface and cross-section scanning electron micrographs of the above oxide films are shown in Fig. 5. The oxide films consist of 0.1–0.2  $\mu\text{m}$  ellipsoidal oxide particles and the heat treatment at 800 °C causes sintering of the particles of the  $\text{La}(\text{Cr}_{0.5}\text{Mn}_{0.5})\text{O}_3$  film. On the quartz glass substrate, some microcracks were

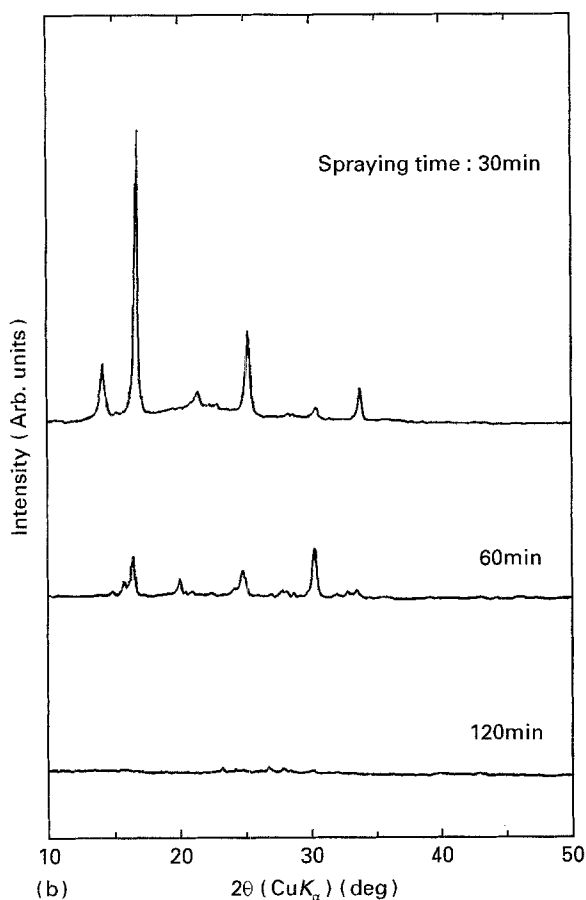
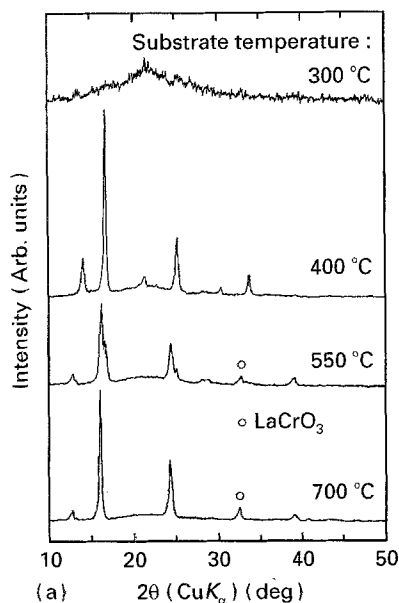


Figure 3 (a) Effect of substrate temperature (spraying time 30 min), and (b) spraying time (substrate temperature 400 °C) on the structure of La(III)-Cr(VI) precursor films formed on quartz glass with 0.15 mol dm<sup>-3</sup> solutions.

observed due to differences in the thermal expansion coefficients,  $\beta$ , of the oxide films ( $\beta = 9.48 \times 10^{-6} \text{ K}^{-1}$  at 350–1000 °C for LaCrO<sub>3</sub> [20],  $\beta = 9.5 \times 10^{-6} \text{ K}^{-1}$  at 800 °C for LaMnO<sub>3</sub> [21]) and quartz glass ( $\beta = 5.6 \times 10^{-7} \text{ K}^{-1}$ ). No cracks were observed on YSZ plate ( $\beta = 10.30 \times 10^{-6} \text{ K}^{-1}$  at 350–1000 °C [20]). The thickness is nearly the same for films formed under the same conditions. The effect of spraying time on the thickness of LaCrO<sub>3</sub> film is shown in

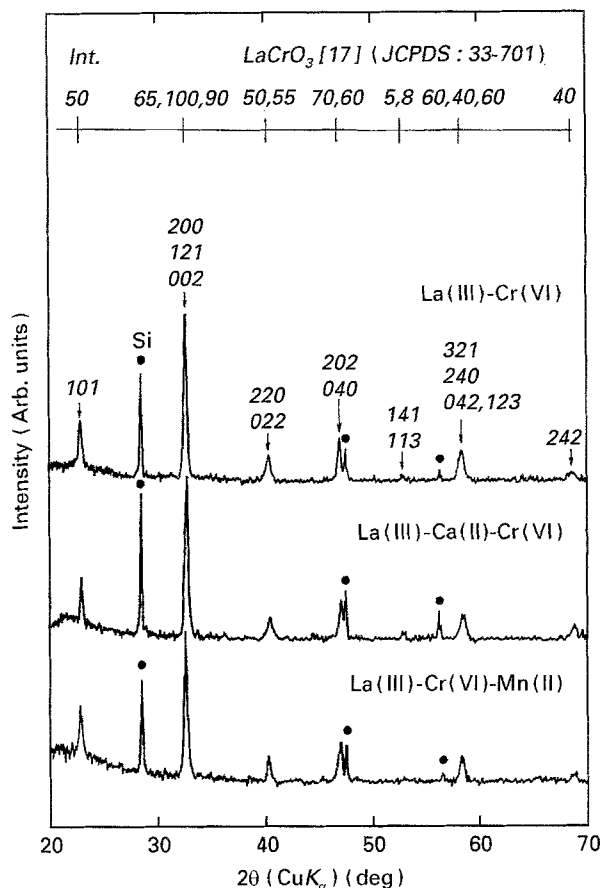


Figure 4 The X-ray diffraction patterns of oxide films formed on quartz glass. The precursor films were formed at 350 °C for 60 min with 0.10 mol dm<sup>-3</sup> solutions.

Fig. 6. It is proportional to spraying time, and the formation rate is about 3  $\mu\text{m h}^{-1}$  at 350 °C. The rate, however, decreased with increasing substrate temperature and was about 1.2  $\mu\text{m h}^{-1}$  at 400 °C.

### 3.3. Electronic conductivity of the oxide films

Temperature dependence of conductivity is shown in Fig. 7 for LaCrO<sub>3</sub>, (La<sub>0.8</sub>Ca<sub>0.2</sub>)CrO<sub>3</sub>, and La(Cr<sub>0.5</sub>Mn<sub>0.5</sub>)O<sub>3</sub> films, for three-cycle and one-cycle formation films. In one-cycle films, LaCrO<sub>3</sub> and La(Cr<sub>0.5</sub>Mn<sub>0.5</sub>)O<sub>3</sub> have very similar conductivity and it increases rapidly with temperatures above 1000 °C. (La<sub>0.8</sub>Ca<sub>0.2</sub>)CrO<sub>3</sub> has much higher conductivity at low temperatures. The conductivity was independent of the thickness and measured values were smaller than the reported ones by two or three orders of magnitude [22–24]. This may be caused by cracks or be due to the low density of the formed oxide films.

The three-cycle films, however, showed better conductivities than the one-cycle ones especially at low temperatures (Fig. 7). The number of cracks was lower, however, an increase in the densities by the three-cycle formation was not confirmed with the cross-sectional observations by SEM.

## 4. Conclusion

Precursor films to lanthanum chromium oxide films were obtained on different substrates by ultrasonic

TABLE I Lattice constants of the formed oxide films

Oxide	Lattice constants (nm)		
	<i>a</i>	<i>b</i>	<i>c</i>
LaCrO <sub>3</sub>			
Film <sup>a</sup>	0.5476 (2)	0.5515 (2)	0.7749 (2)
Powder [18] <sup>b</sup>	0.5480	0.5515	0.7758
Powder [19] <sup>a</sup>	0.54861 (4)	0.55206 (4)	0.77742 (8)
(La <sub>0.8</sub> Ca <sub>0.2</sub> )CrO <sub>3</sub>			
Film	0.5472 (3)	0.5511 (4)	0.7731 (8)
Powder [18]	0.5473	0.5506	0.7752
La(Cr <sub>0.5</sub> Mn <sub>0.5</sub> )O <sub>3</sub>			
Film	0.5481 (1)	0.5518 (1)	0.7765 (3)
Powder [19]	0.54806 (2)	0.55229 (2)	0.77657 (3)

<sup>a</sup>Standard deviations are in parentheses and refer to the last digit.

<sup>b</sup>Accuracy  $\pm 0.0001$  nm.

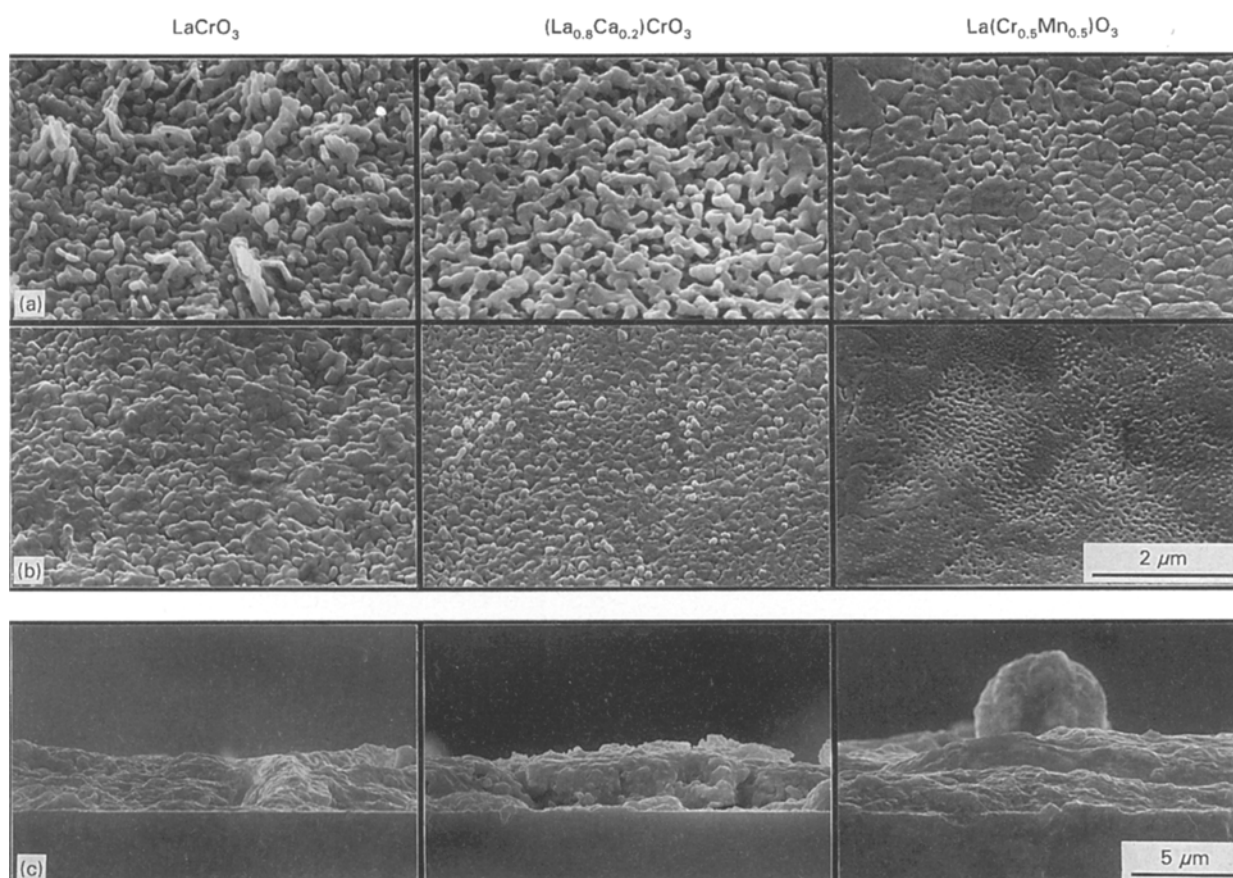


Figure 5 Scanning electron micrographs of the oxide films in Fig. 4; (a,c) on quartz glass and (b) on YSZ plate.

spray pyrolysis of chromate solutions containing lanthanum nitrate, calcium nitrate, and manganese (II) nitrate. There was an optimum substrate temperature for the formation of precursor films, at which uniform dry films were formed with the maximum deposition rate. The composition of the precursor to LaCrO<sub>3</sub> was considered to be La(CrO<sub>4</sub>)(NO<sub>3</sub>)<sub>n</sub>·*n*H<sub>2</sub>O from ICP–AES, TG–DTA, IR measurements, and elemental analysis. The

precursor films were converted to thin films of perovskite-type LaCrO<sub>3</sub>, (La<sub>0.8</sub>Ca<sub>0.2</sub>)CrO<sub>3</sub>, and La(Cr<sub>0.5</sub>Mn<sub>0.5</sub>)O<sub>3</sub> by heat treatment at 800–1000 °C in a nitrogen atmosphere. The composition of the formed oxide films was proportional to that of the solution used for spraying. Repetition of the spray pyrolysis and the heat treatment in nitrogen improved the electronic conductivity of the oxide films.

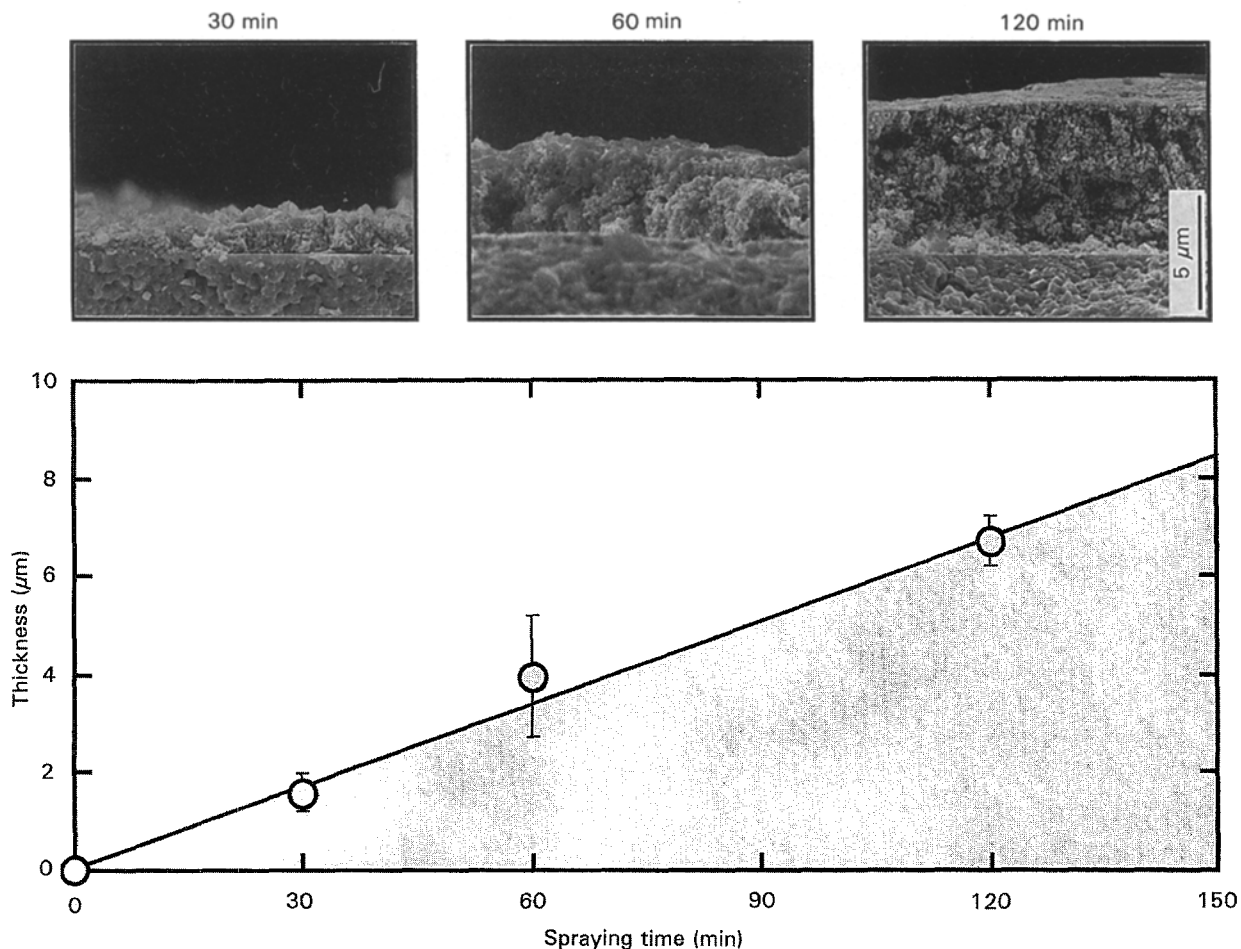


Figure 6 Effect of spraying time on the thickness of  $\text{LaCrO}_3$  films formed on YSZ plates. The precursor films were formed at  $350^\circ\text{C}$  with  $0.10 \text{ mol dm}^{-3}$  solutions.

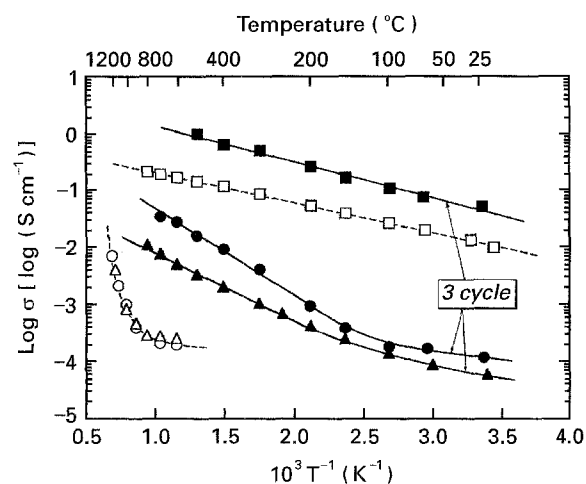


Figure 7 Electronic conductivity of oxide films measured in  $12 \text{ cm}^3 \text{ min}^{-1}$  air flow for (—) three-cycle formation, and (---) one-cycle formation: (○, ●)  $\text{LaCrO}_3$ , (□, ■)  $(\text{La}_{0.8}\text{Ca}_{0.2})\text{CrO}_3$ , (△, ▲)  $\text{La}(\text{Cr}_{0.5}\text{Mn}_{0.5})\text{O}_3$ . The precursor films were formed on  $\text{Si}_3\text{N}_4$  plates at  $350^\circ\text{C}$  for 60 min with  $0.10 \text{ mol dm}^{-3}$  solutions.

### Acknowledgements

The authors thank Mr. Nodasaka and Dr Kodaira of Hokkaido University for the SEM and XRD analyses. Part of this work was carried out under the Visiting Researcher's Programme of Institute for Materials Research, Tohoku University, and by the Grant-in-

Aid for Scientific Research (04650637 and 06452330) from the Ministry of Education, Japan.

### References

1. M. L. NIELSEN, P. M. HAMILTON and R. J. WALSH, in "Ultrafine Particles", edited by W. E. Kuhn (Wiley, New York, 1963) p. 181.
2. H. IMAI, K. TAKAMI and M. NAITO, *Mater. Res. Bull.* **19** (1984) 1293.
3. G. BLANDENET, M. COURT and Y. LAGARDE, *Thin Solid Films* **77** (1981) 81.
4. S. P. S. ARYA and H. E. HINTERMANN, *ibid.* **193/194** (1990) 841.
5. M. LANGLET, E. SENET, J. L. DESCHANVRES, G. DELABOUGLISE, F. WEISS and J. C. JOUBERT, *J. Less-Common Metals* **151** (1989) 399.
6. *Idem*, *Thin Solid Films* **174** (1989) 263.
7. W. J. DESISTO, R. L. HENRY and M. OSOFSKY, *ibid.* **206** (1991) 128.
8. J. L. DESCHANVRES, M. LANGLET and J. C. JOUBERT, *ibid.* **175** (1989) 281.
9. T. SETOGUCHI, M. SAWANO, K. EGUCHI and H. ARAI, *Solid State Ionics* **40/41** (1990) 502.
10. B. GHARBAGE, M. HENAUULT, T. PAGNIER and A. HAMMOU, *Mater. Res. Bull.* **26** (1991) 1001.
11. R. STAUT and P. E. D. MORGAN, US Pat. 3974108, 10 August 1976.
12. H. KONNO, M. TOKITA, S. KITAZAKI and R. FURUICHI, *J. Surf. Finish. Soc. Jpn* **40** (1989) 825.
13. H. KONNO, M. TOKITA and R. FURUICHI, *J. Electrochem. Soc.* **137** (1990) 361.

14. H. KONNO, M. TOKITA, A. FURUSAKI and R. FURUICHI, *Electrochim. Acta* **37** (1992) 2421.
15. A. FURUSAKI, H. KONNO and R. FURUICHI, *Nippon Kagaku Kaishi* **6** (1992) 612.
16. H. KONNO, H. TACHIKAWA, A. FURUSAKI and R. FURUICHI, *Anal. Sci.* **8** (1992) 641.
17. JCPDS 33-701 (1981).
18. S. SONG, M. YOSHIMURA and S. SOMIYA, *J. Mater. Sci. Soc. Jpn* **19** (1982) 49.
19. R. KOC, H. U. ANDERSON and S. A. HOWARD, in "Proceedings, of the 1st International Conference on Solid Oxide Fuel Cells", edited by S. C. Singhal (Electrochemical Society, New Jersey, 1989) p. 220.
20. S. SRILOMSAK, D. P. SCHILLING and H. U. ANDERSON, *ibid.*, p. 129.
21. A. HAMMOUCHE, E. SIEBERT and A. HAMMOU, *Mater. Res. Bull.* **24** (1989) 367.
22. T. KUMAGAI, H. YOKOTA, Y. SHINDO, W. KONDO and S. MIZUTA, *Denki Kagaku* **55** (1987) 269.
23. L. G. J. DE HAART, R. A. KUIPERS, K. J. DE VRIES and A. J. BURGGRAAF, *J. Electrochem. Soc.* **138** (1991) 1970.
24. S. YAMADA, S. NENNO, Y. MATSUMOTO, N. IN-DAYANINGSIH, J. HOMBO, E. SATO, T. SHIRAKASHI and S. YOSHIHARA, *Denki Kagaku* **62** (1994) 246.

*Received 22 April  
and accepted 14 November 1994*